Estimation of ligament strains and joint moments in the ankle during a supination sprain injury

Journal:	*Computer Methods in Biomechanics and Biomedical Engineering*
Manuscript ID:	GCMB-2012-0287.R3
Manuscript Type:	Original Article
Date Submitted by the Author:	22-Jan-2013
Complete List of Authors:	Wei, Feng; Rehabilitation Institute of Chicago, Fong, Daniel; The Chinese University of Hong Kong, Chan, Kai-Ming; The Chinese University of Hong Kong, Haut, Roger; Michigan State University,
Keywords:	Anterior talofibular ligament, Ankle inversion sprain, Injury mechanism, Ankle biomechanics, Computational model, Dynamic simulation

RESPONSES TO REVIEWERS' COMMENTS:

Manuscript ID GCMB-2012-0287.R2 (Computer Methods in Biomechanics and Biomedical Engineering): **Estimation of ligament strains and joint moments in the ankle during a supination sprain injury**

We have revised the manuscript to address the reviewer's last concern. In the revised manuscript we first accepted all the changes made to address the reviewers' previous comments. We then tracked the new changes that directly respond to the reviewer's last critical comment. We want to thank the reviewer for the insightful suggestions that have made this work better.

Reviewer(s)' Comments to Author:

Reviewer: 1

Comments to the Corresponding Author

Effect of variation on results of the value of the damping coefficient values must be added. Justification for not doing so, based on the existing study in the literature (lines 207-210) is not sufficient since that study looked at end range of motion where time effects (and thus damping) were not in play. This is not valid in your study.

We have varied the damping coefficient up and down one order of magnitude (similar to the study by Majors and Wayne, Ann Biomed Eng 39, 2807-2815, 2011) and found that joint moment calculated in the model changed by 0.45 Nm, approximately 2% of the maximum moment (23 Nm) generated in the simulation. In addition, we have also varied the stiffness and the exponent up and down one order of magnitude individually, just like Majors and Wayne (2011) in their study. The results showed that the joint moment was affected by approximately 1.5% and 4.3%, respectively. All these analyses, however, provided no change in the strain results calculated in the model. We therefore believe that ligament strains, generated in linear elastic spring elements, were primarily affected by the prescribed bone motions in the current study, not by the contact parameters. We have included these analyses and results in Discussion of the revised manuscript on page 9, lines 205-214. Again, we would like to thank the reviewer for the suggestions that have made this study more informative.

Estimation of ligament strains and joint moments in the ankle during a supination sprain injury

Feng Wei[1,2], Daniel Tik-Pui Fong[3,4], Kai-Ming Chan[3,4], Roger C. Haut[5]

[1]Sensory Motor Performance Program
Rehabilitation Institute of Chicago
Chicago, IL 60611

[2]Department of Physical Medicine and Rehabilitation
Northwestern University Feinberg School of Medicine
Chicago, IL 60611

[3]Department of Orthopaedics and Traumatology
Prince of Wales Hospital
Faculty of Medicine, The Chinese University of Hong Kong
Hong Kong, China

[4]The Hong Kong Jockey Club Sports Medicine and Health Sciences Center
Faculty of Medicine, The Chinese University of Hong Kong
Hong Kong, China

[5]Orthopaedic Biomechanics Laboratories
Michigan State University
East Lansing, MI 48824

Corresponding Author:
Prof Daniel Tik-Pui Fong
Department of Orthopaedics and Traumatology
Prince of Wales Hospital
Faculty of Medicine, The Chinese University of Hong Kong
Hong Kong, China
Tel: (852) 2632 3535, Email: dfong@ort.cuhk.edu.hk

Word Count: 23420

ABSTRACT

This study presents the ankle ligament strains and ankle joint moments during an accidental injury event diagnosed as a grade I anterior talofibular ligament (ATaFL) sprain. A male athlete accidentally sprained his ankle while performing a cutting motion in a laboratory setting. The kinematics data were input to a three-dimensional rigid-body foot model for simulation analyses. Maximum strains in 20 ligaments were evaluated in simulations that investigated various combinations of the reported ankle joint motions. Temporal strains in the ATaFL and the calcaneofibular ligament (CaFL) were then compared and the three-dimensional ankle joint moments were evaluated from the model. The ATaFL and CaFL were highly strained when the inversion motion was simulated (10% for ATaFL and 12% for CaFL). These ligament strains were increased significantly when either or both plantarflexion and internal rotation motions were added in a temporal fashion (up to 20% for ATaFL and 16% for CaFL). Interestingly, at the time strain peaked in the ATaFL, the plantarflexion angle was not large but apparently important. This computational simulation study suggested that an inversion moment of approximately 23 Nm plus an internal rotation moment of approximately 11 Nm and a small plantarflexion moment may have generated a strain of 15-20% in the ATaFL to produce a grade I ligament injury in the athlete's ankle. This injury simulation study exhibited the potentially important roles of plantarflexion and internal rotation, when combined with a large inversion motion, to produce a grade I ATaFL injury in the ankle of this athlete.

KEYWORDS: Anterior talofibular ligament, Ankle inversion sprain, Injury mechanism, Ankle biomechanics, Computational model, Dynamic simulation.

INTRODUCTION

Ankle sprain is a common sports trauma (Fong et al., 2007). Over 80% of these injuries are caused by excessive ankle joint supination which ruptures lateral ankle ligaments. Studies have been conducted to describe the kinematics of accidental ankle sprains using motion or video analysis (Kristianslund et al., 2011; Mok et al., 2011). These studies, however, do not provide data on ankle ligament strains. Additionally, it has been suggested that deviation of the ground reaction force away from the ankle joint center may result in an explosive ankle joint moment causing injury (Fong et al., 2009a). Such a moment would trigger a twisting motion to stretch ligaments vigorously (Delahunt et al., 2006).

An investigation by Fong et al. (2009b) of a grade I supination injury to the anterior talofibular ligament (ATaFL) has revealed that, in addition to plantarflexion and rearfoot inversion, internal rotation of the foot was noted to be greater than previously reported (Bahr et al., 1998). However, the roles of inversion, plantarflexion, and internal rotation, or their temporal combination on lateral ligament strains are still unclear. Recently, Wei et al. (2011b) has developed a computational model and utilized motion analysis-based kinematic data from laboratory tests to drive the model for estimations of dynamic ankle ligament strains and joint moments (Wei et al., 2011a). The model has shown its ability to help in the study of the motions that may predispose ankle ligaments to injury during external foot rotation. The purpose of the current study was to use this model to study the motions producing ankle ligament strains and joint moments during the accidental sprain event documented by Fong et al. (2009b). Since the injury was diagnosed as a grade I ATaFL sprain, and a combination of inversion, plantarflexion,

and internal rotation has been documented, a high strain in this ligament and high joint moments in these three directions were expected.

METHODS

Injury case

A male athlete (23 years, 1.75 m, 62.6 kg) wore a pair of high-top basketball shoes and performed a series of cutting motion trials in the laboratory. In one trial the athlete accidentally sprained his right ankle, and the injury was immediately diagnosed as a grade I sprain of the ATaFL by a well-trained orthopaedic specialist (K.M.C.). The injury occurred in the laboratory that utilized marker-based motion and model-based image-matching video analysis systems (Fong et al., 2009b).

Computational modeling

A 3D multi-body dynamic foot model (Wei et al., 2011b) was utilized for simulations of the injury event. The model comprised five segments, namely the tibia, fibula, talus, calcaneus, and tarsal and metatarsal bones. Details of model development and validation have been previously described (Wei et al., 2011b). The model was constructed from a generic cadaver ankle (male, 19 years, 1.88 m, 86 kg) which was scanned using computed tomography (CT) in a neutral position and with a separation of 0.6 mm between slices. CT images were converted into 3D models in MIMICS (Materialise, Ann Arbor, MI) and imported into dynamic rigid-body motion simulation software (SolidWorks, TriMech Solutions, LLC, Columbia, MD) (Iaquinto and Wayne, 2010; Liacouras and Wayne, 2007). The neutral position of the ankle from the CT scan was maintained in the model. The model includes 20 ligaments formulated as linear elastic, tension only springs (Figure 1) with their stiffnesses (N/mm) adapted from the literature (Table 1). The slack length

of the ligaments was defined with the model positioned in neutral. An initial strain of 2%, implemented by inserting a spring element of length 2% shorter than the initial length (distance between insertion points), was assigned to each ankle ligament (Wei et al., 2011a), thereby inducing an *in situ* preload in the ligament. An initial strain of 0.5%, however, was applied to the interosseous ligaments (Liacouras and Wayne, 2007). The ground was simulated as a rigid platform in the software. The 3D contacts (Iaquinto and Wayne, 2010) were implemented between adjacent bones as well as between the bones and ground plate in order to prevent overlap during the simulation. This was done by calculating the interference at each time step and applying an outward force if any overlap was detected. The magnitude of the force F was a function of material stiffness k (10,000 N/mm), penetration depth g, exponent e (1.75), penetration velocity, and damping coefficient c (400 Ns/mm), with the penetration at maximum damping set to its lowest allowable value (d = 0.001 mm).

$$F = kg^{e} + \left(\frac{dg}{dt}\right) f(c,d)$$

Friction was neglected to simulate cartilage effects. In the model the tibia was only allowed to move vertically (one degree of freedom). The fibula, talus, and calcaneus were allowed to move in all six degrees of freedom, leaving bone motion to be a function of ligament behavior, surface contact, and external perturbations. For simplification purposes, the remaining bones of the foot (tarsal and metatarsal bones) were fused together and moved as a unit, with its motion primarily dependent on motions of the talus and calcaneus.

Injury simulation

At the beginning of the simulation, three times body weight (1840 N) was applied to the proximal end of the model to simulate dynamic weight bearing (Cavanagh and Lafortune, 1980), distributing one-sixth of the load on the fibula and the rest on the tibia (Lambert, 1971; Wei et al., 2011b). The 3D, temporal kinematic data from the case report (Fong et al., 2009b), i.e. inversion-time data, plantarflexion-time data, and internal rotation-time data, were used as input for simulations (Wei et al., 2011a). These actual motions placed the neutral foot model in the starting position of the athlete's ankle in order to begin the simulation. Three motor elements were used to drive the motion of the bones, two on the talus for plantarflexion and internal rotation, respectively, and one on the calcaneus for inversion. The three axes of rotation were set as: (1) dorsi-plantarflexion – fixed to the talus through its estimated center and initially oriented medial-lateral; (2) internal-external rotation – along the tibial axis; and (3) inversion-eversion – fixed to the calcaneus through its estimated center and perpendicular to the previous two (initially oriented anteroposterior) (Figure 1). These axes of rotation were based on a joint coordinate system (Wu et al., 2002), as the same system was utilized to calculate the injurious kinematics (Fong et al., 2009b). To systematically investigate the contribution of each motion and their combinations, four motion simulations were performed: (1) pure inversion; (2) inversion plus plantarflexion; (3) inversion plus internal rotation; and (4) a combination of inversion, plantarflexion, and internal rotation. The SolidWorks Motion package from the simulation software was used to execute these simulations. Continuous rotation-time data were interpolated (using the Akima Spline method) into the SolidWorks Motion to drive the talus and/or the calcaneus movement. Ligament strains were estimated from the model (Iaquinto and Wayne, 2011; Wei et al., 2011b). Resistive moments, deduced by inverse dynamics from the motors along the three axes of rotation, were also obtained from the model analysis.

RESULTS

Under inversion alone, the CaFL was strained the most at 12% (Figure 2). The ATaFL and LTaCL were strained to approximately 10%. When temporal plantarflexion or internal rotation was added, both the CaFL and ATaFL were strained to approximately 14-16%. With all three motions combined the ATaFL was strained the most at 20% followed by the CaFL at 16%. Temporal strain profiles of the ATaFL and CaFL were compared, along with the foot motions and ankle joint moments (Figure 3). There was a switch in magnitude of strains from the CaFL to the ATaFL at 0.16 s after footstrike (heel strike). The highest moment was 23 Nm for inversion followed by 11 Nm for internal rotation (Figure 3c).

DISCUSSION

A grade I ankle sprain is characterized as minimal tearing of ligament fibers (Noyes et al., 1989). Rupture strain of ankle ligaments can be estimated in the range of 30-35% (Beumer et al., 2003; Funk et al., 2000). Ligament collagen fibers are thought to tear when half of the rupture strain is reached (Yahia et al., 1990). The ATaFL strain in the current study reached 15-20%, which is approximately one-half of the suggested rupture strain. Previous studies also report that a 10 Nm external moment applied to the foot will cause pain and discomfort, and an external moment of 41-45 Nm generates ankle fractures (Markolf et al., 1989). By investigating a supination injury case, the current study indicated that an ankle joint moment up to 23 Nm may produce a grade I ankle sprain.

Clinically the mechanism of an ankle supination sprain has been associated with a combination of inversion and plantarflexion. In contrast, Kristianslund et al. (2011) and Mok et al. (2011) suggest the important role of internal rotation. Mok et al. (2011) also suggest that future designs of injury prevention measures may only need to consider inversion and internal rotation. Yet, the current study showed that either plantarflexion or internal rotation, when added to inversion, increased the ATaFL strains from 10% to approximately 15-16%. And the temporal combination of all three motions raised the ATaFL strain to over 20% (Figure 2), suggesting that, in addition to inversion, both plantarflexion and internal rotation may be important in generating supination ankle sprains, as estimated by this one case study.

While a few studies have presented constant stiffnesses for ankle ligaments (Attarian et al., 1985; Siegler et al., 1988), nonlinear and viscoelastic behavior in those ligaments has been observed (Attarian et al., 1985; Funk et al., 2000). Ankle ligament strains under a physiological range of ankle motion are thought to be in the range of 5-10% (Colville et al., 1990; Ozeki et al., 2002). Funk et al. (2000) reported the ankle ligament force-strain curves have a typical toe region up to 6% strain followed by a loading region (nearly linear) up to 20% strain. Although the linear approximation used in the current study may have underestimated ankle ligament strains, the error was likely minimal (within 3%) for a strain range of 16-20%, while larger errors (up to 50%) could be involved for strains less than 15% (Funk et al., 2000). Additionally, a previous study by others has concluded that a viscoelastic assumption of the ankle ligaments could be neglected for very slow (< 0.0001/s) or very fast (> 1/s) strain rates, but substantial effects may exist on ligament behavior for intermediate strain rates (Funk et al., 2000). The modeled

ligaments in the current study experienced strain rates approximately in the range of 1-1.5/s, implying that the viscoelasticity of those ligaments may be negligible.

Other assumptions of the model and the simulation should also be noted. Firstly, the tarsal and metatarsal bones were fused together and moved as a unit in the model for simplification purposes. Although the ligaments connecting the tarsal and metatarsal bones may be less important than those listed in Table 1, this fusion could have caused an overestimation of the joint moments calculated from the model, especially for the internal rotation moment. Secondly, model sensitivity to the parameters chosen to define the contact was evaluated by individually varying the stiffness, exponent, and damping coefficient up and down one order of magnitude, similar to a previous study by others ~~the impact of damping coefficients, chosen to define the contact, on bone motion and ligament strain was not investigated in the current study. However a recent study, by others, using a similar modeling approach to study the wrist biomechanics varies the contact parameters up and down one order of magnitude and concludes little (< 1%) to no change in range of motion of the wrist predicted by the model~~ (Majors and Wayne, 2011). Joint moment was most affected by the exponent term (4.3%) followed by the damping parameter (2.0%) and the stiffness value (1.5%). Varying these parameters provided no change in the ligament strain results predicted by the model. Thirdly, a constant weight bearing load was used in the current study due to the unavailability of ground reaction force (GRF) data from the case report. In addition, this constant load was applied in the beginning of simulation, not at heelstrike, because the time for the GRF to reach its maximum was unknown. Future experimental studies with use of a force plate may provide detailed GRF data (both magnitude and duration) so that a simulated weight bearing load could be applied at footstrike. Finally, the

effect of a lack of the proximal tibiofibular joint in the model on potential alterations of the ankle stability is currently unknown.

While this computational ankle model has provided insights into motions responsible for ankle injury by simulating both *in vitro* (Wei et al., 2012; Wei et al., 2010) and *in vivo* experiments (Wei et al., 2011a), it has been based on only a generic model, without potential effects of the musculature. Therefore joint moments may have been underestimated (Wei et al., 2011a). Additionally, the effects of anatomical differences between the injured subject and the cadaver ankle used to build the model are unknown. Future studies that investigate ankle injury mechanisms and prevention strategies may want to build subject-specific models, incorporate muscle effects, and potentially integrate the nonlinear and viscoelastic responses of ankle ligaments.

ACKNOWLEDGEMENTS

The authors thank Dr. Seungik Baek from Michigan State University for providing the MIMICS software.

REFERENCES

Attarian DE, McCrackin HJ, DeVito DP, McElhaney JH, Garrett WE, Jr. 1985. Biomechanical characteristics of human ankle ligaments. *Foot Ankle* 6(2):54-58.

Bahr R, Pena F, Shine J, Lew WD, Engebretsen L. 1998. Ligament force and joint motion in the intact ankle: a cadaveric study. *Knee Surg Sports Traumatol Arthrosc* 6(2):115-121.

Beumer A, van Hemert WL, Swierstra BA, Jasper LE, Belkoff SM. 2003. A biomechanical evaluation of the tibiofibular and tibiotalar ligaments of the ankle. *Foot Ankle Int* 24(5):426-429.

Cavanagh PR, Lafortune MA. 1980. Ground reaction forces in distance running. *J Biomech* 13(5):397-406.

Colville MR, Marder RA, Boyle JJ, Zarins B. 1990. Strain measurement in lateral ankle ligaments. *Am J Sports Med* 18(2):196-200.

Delahunt E, Monaghan K, Caulfield B. 2006. Altered neuromuscular control and ankle joint kinematics during walking in subjects with functional instability of the ankle joint. *Am J Sports Med* 34(12):1970-1976.

Fong DT, Chan YY, Mok KM, Yung P, Chan KM. 2009a. Understanding acute ankle ligamentous sprain injury in sports. *Sports Med Arthrosc Rehabil Ther Technol* 1:14.

Fong DT, Hong Y, Chan LK, Yung PS, Chan KM. 2007. A systematic review on ankle injury and ankle sprain in sports. *Sports Med* 37(1):73-94.

Fong DT, Hong Y, Shima Y, Krosshaug T, Yung PS, Chan KM. 2009b. Biomechanics of supination ankle sprain: a case report of an accidental injury event in the laboratory. *Am J Sports Med* 37(4):822-827.

Funk JR, Hall GW, Crandall JR, Pilkey WD. 2000. Linear and quasi-linear viscoelastic characterization of ankle ligaments. *J Biomech Eng* 122(1):15-22.

Iaquinto JM, Wayne JS. 2010. Computational model of the lower leg and foot/ankle complex: application to arch stability. *J Biomech Eng* 132(2):021009.

Iaquinto JM, Wayne JS. 2011. Effects of surgical correction for the treatment of adult acquired flatfoot deformity: a computational investigation. *J Orthop Res* 29(7):1047-1054.

Kristianslund E, Bahr R, Krosshaug T. 2011. Kinematics and kinetics of an accidental lateral ankle sprain. *J Biomech* 44(14):2576-2578.

Lambert KL. 1971. The weight-bearing function of the fibula. A strain gauge study. *J Bone Joint Surg Am* 53(3):507-513.

Liacouras PC, Wayne JS. 2007. Computational modeling to predict mechanical function of joints: application to the lower leg with simulation of two cadaver studies. *J Biomech Eng* 129(6):811-817.

Majors BJ, Wayne JS. 2011. Development and validation of a computational model for investigation of wrist biomechanics. *Ann Biomed Eng* 39(11):2807-2815.

Markolf KL, Schmalzried TP, Ferkel RD. 1989. Torsional strength of the ankle in vitro. The supination-external-rotation injury. *Clin Orthop Relat Res* (246):266-272.

Mok KM, Fong DT, Krosshaug T, Engebretsen L, Hung AS, Yung PS, Chan KM. 2011. Kinematics analysis of ankle inversion ligamentous sprain injuries in sports: 2 cases during the 2008 Beijing Olympics. *Am J Sports Med* 39(7):1548-1552.

Noyes FR, Grood ES, Torzilli PA. 1989. Current concepts review. The definitions of terms for motion and position of the knee and injuries of the ligaments. *J Bone Joint Surg Am* 71(3):465-472.

Ozeki S, Yasuda K, Kaneda K, Yamakoshi K, Yamanoi T. 2002. Simultaneous strain measurement with determination of a zero strain reference for the medial and lateral ligaments of the ankle. *Foot Ankle Int* 23(9):825-832.

Pfaeffle HJ, Tomaino MM, Grewal R, Xu J, Boardman ND, Woo SL, Herndon JH. 1996. Tensile properties of the interosseous membrane of the human forearm. *J Orthop Res* 14(5):842-845.

Siegler S, Block J, Schneck CD. 1988. The mechanical characteristics of the collateral ligaments of the human ankle joint. *Foot Ankle* 8(5):234-242.

Wei F, Braman JE, Weaver BT, Haut RC. 2011a. Determination of dynamic ankle ligament strains from a computational model driven by motion analysis based kinematic data. *J Biomech* 44(15):2636-2641.

Wei F, Hunley SC, Powell JW, Haut RC. 2011b. Development and validation of a computational model to study the effect of foot constraint on ankle injury due to external rotation. *Ann Biomed Eng* 39(2):756-765.

Wei F, Meyer EG, Braman JE, Powell JW, Haut RC. 2012. Rotational stiffness of football shoes influences talus motion during external rotation of the foot. *J Biomech Eng* 134(4):041002.

Wei F, Villwock MR, Meyer EG, Powell JW, Haut RC. 2010. A biomechanical investigation of ankle injury under excessive external foot rotation in the human cadaver. *J Biomech Eng* 132(9):091001.

Wu G, Siegler S, Allard P, Kirtley C, Leardini A, Rosenbaum D, Whittle M, D'Lima DD, Cristofolini L, Witte H, Schmid O, Stokes I. 2002. ISB recommendation on definitions of

joint coordinate system of various joints for the reporting of human joint motion--part I: ankle, hip, and spine. International Society of Biomechanics. *J Biomech* 35(4):543-548.

Yahia L, Brunet J, Labelle S, Rivard CH. 1990. A scanning electron microscopic study of rabbit ligaments under strain. *Matrix* 10(1):58-64.

FIGURE LEGENDS

Figure 1: Posterior (a), medial (b), and lateral (c) views of the ankle model showing the axes of rotation used in the simulations (dotted lines in a and b) and the locations of 16 simulated ligaments (c): the interosseous ligaments (IOL-I and IOL-II); the anterior and posterior tibiofibular (ATiFL and PTiFL); the calcaneofibular (CaFL); the anterior and posterior talofibular (ATaFL and PTaFL); the anterior and posterior tibiotalar (ATiTL and PTiTL); the tibionavicular (TiNL); the talonavicular (TaNL); the calcaneocuboid (CaCL); the calcaneonavicular (CaNL); the medial, central, and lateral plantar fascia (MPF, CPF, and LPF). For clarity, the lateral, interosseous, medial, and posterior talocalcaneal ligaments (LTaCL, ITaCL, MTaCL, and PTaCL) between the talus and the calcaneus were set invisible. Ligament initial length and stiffness were documented in Table 1.

Figure 2: Maximum strains estimated from the model in various selected ligaments (> 2% strain) for different ankle motions.

Figure 3: Normalized kinematic data from Fong et al. (2009b) were re-plotted (a). Values were normalized between their initial and peak measures, i.e. plantarflexion: -23.6º~1.0º; inversion: 15.6º~47.6º; internal rotation: -12.3º~10.0º. Temporal profiles of strains (b) in the ATaFL and CaFL, and ankle joint moments (c) during the injury incident were estimated from the model by applying a combination of inversion, plantarflexion, and internal rotation simultaneously.

TABLE

Table 1: Twenty ligaments were simulated in the model. The initial length was the length prior to the application of an *in situ* strain. The stiffness was adapted from Wei et al. (2011b).

Ligament names	Abbreviation	Initial length (mm)	Stiffness (N/mm)
Interosseous I	IOL-I	18.0	400 (Pfaeffle et al., 1996)
Interosseous II	IOL-II	17.2	400 (Pfaeffle et al., 1996)
Anterior Tibiofibular	ATiFL	18.1	90 (Siegler et al., 1988)
Posterior Tibiofibular	PTiFL	22.7	90 (Beumer et al., 2003)
Calcaneofibular	CaFL	41.3	70 (Liacouras and Wayne, 2007)
Anterior Talofibular	ATaFL	32.2	90 (Siegler et al., 1988)
Posterior Talofibular	PTaFL	18.8	70 (Liacouras and Wayne, 2007)
Anterior Tibiotalar	ATiTL	18.0	70 (Liacouras and Wayne, 2007)
Posterior Tibiotalar	PTiTL	16.0	80 (Liacouras and Wayne, 2007)
Tibionavicular	TiNL	39.3	40 (Siegler et al., 1988)
Talonavicular	TaNL	11.0	70 (Liacouras and Wayne, 2007)
Interosseous Talocalcaneal	ITaCL	8.7	70 (Liacouras and Wayne, 2007)
Lateral Talocalcaneal	LTaCL	12.2	70 (Liacouras and Wayne, 2007)
Medial Talocalcaneal	MTaCL	8.5	70 (Liacouras and Wayne, 2007)
Posterior Talocalcaneal	PTaCL	29.9	70 (Liacouras and Wayne, 2007)
Calcaneocuboid	CaCL	26.2	70 (Liacouras and Wayne, 2007)
Calcaneonavicular	CaNL	26.7	70 (Liacouras and Wayne, 2007)
Medial Plantar Fascia	MPF	147.9	200 (Iaquinto and Wayne, 2010)
Central Plantar Fascia	CPF	146.5	230 (Iaquinto and Wayne, 2010)
Lateral Plantar Fascia	LPF	133.2	180 (Iaquinto and Wayne, 2010)

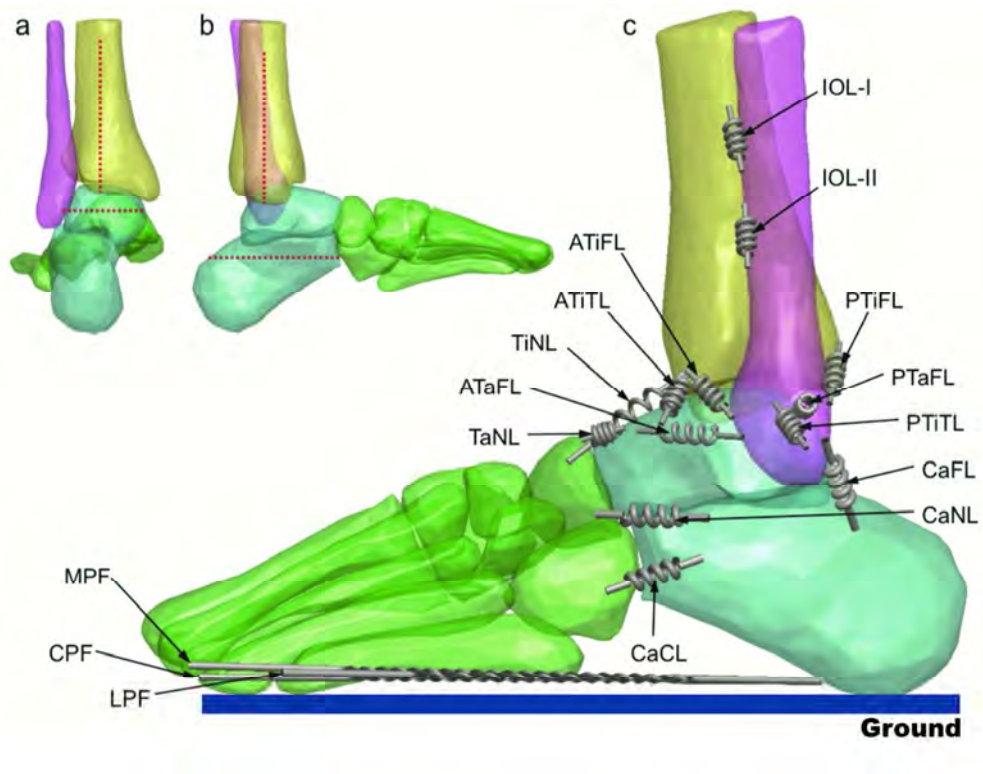

Posterior (a), medial (b), and lateral (c) views of the ankle model showing the axes of rotation used in the simulations (dotted lines in a and b) and the locations of 16 simulated ligaments (c): the interosseous ligaments (IOL-I and IOL-II); the anterior and posterior tibiofibular (ATiFL and PTiFL); the calcaneofibular (CaFL); the anterior and posterior talofibular (ATaFL and PTaFL); the anterior and posterior tibiotalar (ATiTL and PTiTL); the tibionavicular (TiNL); the talonavicular (TaNL); the calcaneocuboid (CaCL); the calcaneonavicular (CaNL); the medial, central, and lateral plantar fascia (MPF, CPF, and LPF). For clarity, the lateral, interosseous, medial, and posterior talocalcaneal ligaments (LTaCL, ITaCL, MTaCL, and PTaCL) between the talus and the calcaneus were set invisible. Ligament initial length and stiffness were documented in Table 1.
127x97mm (300 x 300 DPI)

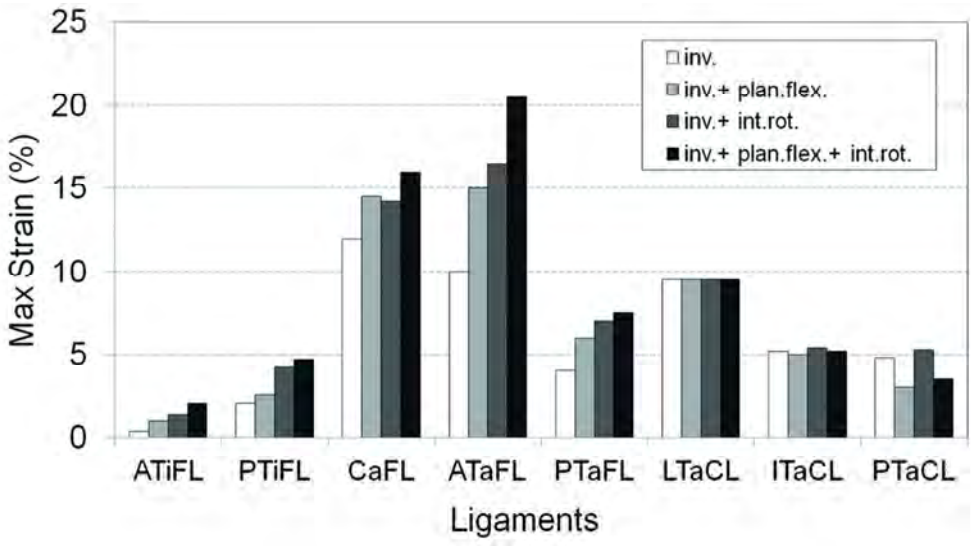

Maximum strains estimated from the model in various selected ligaments (> 2% strain) for different ankle motions.
48x26mm (600 x 600 DPI)

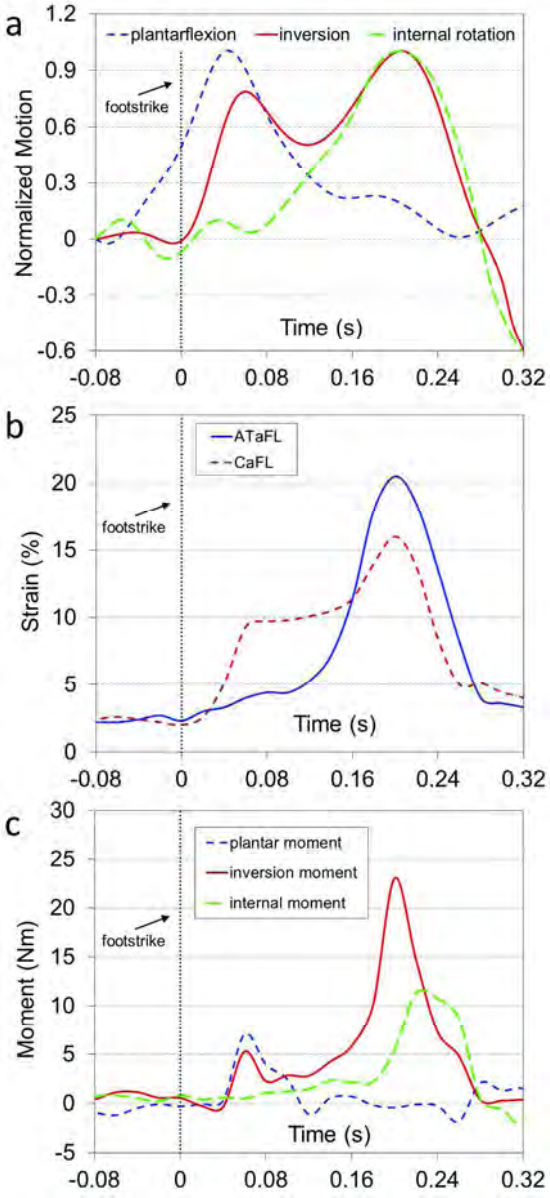

Normalized kinematic data from Fong et al. (2009b) were re-plotted (a). Values were normalized between their initial and peak measures, i.e. plantarflexion: -23.6º~1.0º; inversion: 15.6º~47.6º; internal rotation: -12.3º~10.0º. Temporal profiles of strains (b) in the ATaFL and CaFL, and ankle joint moments (c) during the injury incident were estimated from the model by applying a combination of inversion, plantarflexion, and internal rotation simultaneously.
240x524mm (300 x 300 DPI)